

Surface Roughness Prediction of EDM machined Dies(EN8) using Deep learning

Ghanshyam Patel^a and M.B.Kiran^a

^aDepartment of Mechanical Engineering, School of Technology, Pandit Deendayal Energy University, Gandhinagar, Gujarat, India

ARTICLE HISTORY

ABSTRACT

The die-making industry commonly uses EN8. The dies made by the Electric Discharge Machining (EDM) processes function properly only with the required surface finish. Many previously developed ANN models are used to predict only average roughness R_a . To fully assess the die performance, roughness parameters such as R_z , R_p , R_q , and R_v are also necessary. The present surface roughness prediction model using ANN assumes a special significance in this context. The outcomes are validated by comparing the ANN prediction model and the RSM model outputs. The network trained with the LM algorithm gave the best results while predicting the roughness parameters. MAPE, MSE, and R^2 are used to assess the effectiveness of the proposed model. Experimental investigation revealed that the network architecture (3-15-5) gave the best results. During testing, while predicting R_a , R_q , R_z , R_p , and R_v , the average values obtained for MSE, MAPE, and R^2 were 0.00030, 0.13432, and 0.99974, respectively. Both the predicted values and the experimental results show a good degree of agreement. Consequently, this approach is appropriate for a thorough examination of die surface roughness.

KEYWORDS

Roughness measurement, Electrical Discharge Machining (EDM), Roughness prediction, ANN, and RSM.

1. Introduction

Surface roughness (SR) is a key metric used to assess a machined component's quality. It might be regarded as a gauge of the product's quality. Many aerospace components, such as engine piston heads and landing gear, are manufactured by EDM. It is popular because the desired surface finish can be achieved easily, even with hard-to-machine materials. In this machining process, the component to be machined is connected to the positive terminal and copper or any conductive metal electrode is used as the negative terminal. The process generates enough heat to erode the workpiece. The dielectric liquid will constantly flush out tiny particles from the machined surface to cool metal pieces and electrodes. It also controls the temperature so that the surface is not damaged. Surface roughness is a vital parameter in all industrial applications, including die-making. Many researchers have been applying artificial intelligence (AI) to many fields, including die-making. In this study, we have used three optimizers (LM, BR, and RProp) because of their salient properties and to evaluate them while predicting the surface roughness parameters in EDM machining (Table 1) of dies.

Table 1.: Comaparision of ANN algorithms- LM, Br, RProp

| Training algorithm | trainlm (Levenberg-Marquardt) | trainbr (Bayesian Regularization) | trainrp (Resilient Backpropagation) |
|-------------------------------|------------------------------------|-------------------------------------|---|
| Speed | Fast | Moderate | Slow |
| Memory Usage | High | Moderate | Low |
| Regularization | No | Yes (automatic) | No |
| Generalization | Good | Excellent | Moderate |
| Suitability | Small to medium-sized networks | Noisy data, generalization critical | Large networks, memory-constrained environments |
| Overfitting Control | Requires external techniques | Built-in | Requires external techniques |
| Complexity Handling | Handles less complex problems well | Handles complex and noisy data well | Handles moderate complexity |
| Sensitivity to Initialization | High | Moderate | Low |

A popular method for extracting information from unstructured data is the artificial neural network. The extensive connectivity of neurons used in model-based ANN design enhances performance. The network algorithm uses input, hidden, and output layers. The algorithm determines an initial set of weights and specifies how weights will be applied to improve performance during the training phase. A neuron's reaction to a signal it receives is controlled by an activation function. The sigmoid function is the most frequently utilized activation function. Predicting surface roughness (SR) parameters is the focus of the current study. R_z , R_p , R_v , R_a , and R_q using an AI-based model. Earlier attempts by researchers included only the prediction of R_a as a roughness parameter. For complete characterization of dies require R_q , R_z , R_p , R_v parameters (Table 2) as well. In this context, the current research work assumes special significance.

Table 2.: Influence of different surface roughness parameters on functionality of Dies

| Roughness type | Full Name | Functionality |
|----------------|-------------------------------|---|
| R_a | Arithmetic Average Roughness | A smoother surface (lower R_a) can reduce friction and wear, improving the lifespan and performance of the die. Conversely, a higher R_a can increase friction, leading to more rapid wear and potentially causing defects in the formed parts.. |
| R_q | Root Mean Square Roughness | A lower R_q value indicates a smoother surface. Smoother surfaces typically enhance the performance and longevity of the die, while higher R_q values might increase wear and friction. |
| R_z | Maximum Height of the Profile | High R_z values can indicate deep valleys and high peaks, which can lead to increased material sticking, greater friction, and higher wear rates. Lower R_z values suggest a more uniform surface, beneficial for consistent die performance. |
| R_p | Maximum Peak height | High R_p values can result in localized stress concentrations, which may lead to premature wear or damage to the die. Lower R_p values contribute to a smoother interaction surface, reducing the likelihood of localized damage. |
| R_v | Maximum Valley Depth | Deep valleys (high R_v) can act as stress risers and sites for material buildup or contamination, potentially causing defects in the formed parts and accelerating die wear. Lower R_v values help maintain a more even surface, promoting better die performance. |

2. Literature review

EDM of EN8 die steel was investigated by Anurag et al. [1]. They carried out a number of tests to look into how SR and MRR were affected by wire feed, servo voltage, I_p , T_{on} , and T_{off} . Experimental studies have demonstrated that the EWR is proportional to MRR for higher values of input parameters. Mustafaiz et al. have studied the application of machine learning techniques, including W-ELM, ELM, Q-SVR, and SVR, to predict the SR of aluminium alloy components machined by EDM.[2]. The investigations have revealed W-ELM model gave good results ($0.9720 R^2$) for components produced by the WEDM process. To estimate the MRR and average roughness, Ushasta Aich et al. [3] used high-speed steel in an experiment on an EDM machine and suggested a model based on support vector machines (SVM). To improve the input parameters, they used Particle Swarm Optimization (PSO). The proposed model's efficiency was assessed using mean absolute percentage error (MAPE). They obtained MAPE values of 8.0909 and 7.08 for MRR and R_a , respectively. Balasubramanian et al.[4] investigated NiTi alloy (SMA) in WEDM. The machining parameters of current, servo voltage, T_{on} , angle of cut, and T_{off} were examined using the response surface. It was demonstrated that while servo voltage and T_{off} steadily reduced, R_a increased by 58% and MRR increased by 57% when T_{on} and current increased. An ANN model was created by Milan Kumar Das et al.[5] to forecast the surface roughness of EN 31 steel that has been EDM machined. Average R_a was used as the output neuron, whereas machining parameters were used as input neurons. Various training algorithms, including LM, SCG, and GDX, were employed. The best network was chosen after comparing the results obtained from the above training techniques. Results obtained from the

LM algorithm are good when predicting SR. The ANN model predicted roughness better than the RSM model. In order to study the Adaptive ANFIS and ANN for predicting MRR and SR using membership functions like gaussmf, gauss2mf, and Gbell, Naresh et al.[6] used Nitinol alloy on WEDM machines. The model was developed by Levenberg-Marquardt (LM), Elman, ANFIS, and GRNN algorithms. K.M. Patel et al. [7] did an experiment using components made of ceramic composites. They studied the relationship between the EDM machining parameters T_{on} , V_{gap} , and duty cycle. It is discovered that the primary factor influencing surface roughness is T_{on} . Uma Maheshwera et al.[8] investigated the WEDM machining of Inconel 718. Surface roughness prediction was done using ANN, SVM, and GA. Experiments revealed that ANN and GA gave better results when compared to RSM. ANN model architecture 5-10-10-1 was identified as optimum. Using SVM model prediction, an R-value of 0.99998 and MAPE of 0.0347% were obtained. SVM and Generic Algorithm (GA) helped in the quick and accurate prediction of SR. T. R. Paul et al.[9] used a hybrid technique to study the optimization process parameters utilizing Inconel 800 on EDM. They optimized the EDM process parameters PCA and MOORA. The investigation has revealed that the values of T_{off} , T_{on} , and I_p set to 85 μ s, 300 μ s, and 18A, respectively, gave an optimal performance.

Routara et al.[10] studied the EDM machining characteristics of T6-Al7075. For both rotary and steady tool modes, the parameters T_{on} T_{off} , I_p , and voltage are used. The investigation revealed that MRR increases when the tool operates in rotary mode. Jamal Seedi et al.[11] investigated in an industrial measurement system using a neural network for determining R_a and fault detection on degraded steelwork parts. By combining CNN-based regression with CNN-based classification, they achieved accurate roughness estimation (7.32% error), high defect detection accuracy (97.26%), and precise localization (99.09% area under the ROC). Ranjit Singh et al.[12] used EDM machined Cu-based shape memory alloy to optimize parameters using techniques of the desirability approach, TBLO, GA. This study examines DD and TWR. The DD was decreased by lowering the T_{on} and T_p values. Hatice Varol et al.[13] used the metal alloy Inconel 718 and non-traditional production techniques like EDM. An artificial intelligence model for evaluating R_a based on process parameters was developed using ANN and GEP. The results showed that the GEP method performed lower than the ANN method. The accuracy was 0.66 in the GEP model and R^2 in ANN was 0.93. Yogesh et al.[14] drew attention to the difficulties in determining the ideal parameters for the highest MRR and the lowest R_a as well as the limitations of conventional testing techniques. The suggested approach uses a Decision Tree and Naive Bayes algorithms to forecast R_a , MRR which saves time and important resources. By adjusting the depth of cut, speed, and feed, Ilhan [15] Asilturk et al. investigated surface roughness during turning. The design of the experiment is fully factorial. SR is better determined by the ANN model than by the multiple regression approach. For training data, a neural network model's coefficient of determination (R^2) is 99.8%, while for testing data, it is 99.4%. It is 98.9% in multiple regression models.

Vishal Lalwani et al. [16] proposed a comparison for the WEDM process of prediction models using RSM and ANN for machining of Inconel 718 superalloy. Compared to the ANN model, the RSM model's prediction accuracy was lower. Kumaresha dey [17] suggested a method for Electrical Discharge Turning (EDT). One kind of EDM procedure that involves material removal from cylindrical workpieces is called EDT. More accurate predictions are made by LSTM-based recurrent neural networks, and general regression neural networks are known for their remarkable robustness. An ANN model to predict the SR performance during the end-milling process developed Azlan et al.[18]. The training, learning, performance, and transfer functions are represented by the functions traingdx, learnngdx, MSE, and logsig, respectively. Feedforward backpropagation is chosen as the preferred algorithm. Eight distinct network structures have been utilized in this study: (3-1-1), (3-3-1), (3-6-1), (3-7-1), (3-1-1-1), (3-3-3-1), (3-6-6-1), and (3-7-7-1). It was discovered that the best forecast for the surface roughness performance metric was provided by the (3-1-1) structure. Among the optimization techniques used in artificial intelligence are PSO, TS, GA, SA, and ACO. Amrita et al. [19] used EDM oil and Jatropha to manufacture AISI D2 steel on an EDM. The decision tree, random forest, and linear regression were used to predict SR.

The lowest SR of $4.5\mu\text{m}$ was obtained for EDM and Jatropha oil with current = 9 A, gap voltage = 50V, and $T_{on} = 30 \mu\text{s}$, $T_{off} = 12 \mu\text{s}$. Out of all the strategies, random forest modelling had the highest accuracy, with an MSE of 1.36% and an R^2 value of 0.89. Angelos P. Markopoulos et al. [20] suggested ANN models for EDM SR prediction. Steel grades were used in EDM tests. Two separate applications, Matlab and Netlab were utilized for the ANN formulation and EDM modelling. It has been demonstrated that both Matlab and Netlab models function effectively for EDM. Liborio Cavaleri et al. [21] suggested using the backpropagation network (BPNN) and the multi-layer perceptron to estimate the average surface roughness of surfaces that have been electro-discharge machined, out of the total of the 2880 developed NN models. The 5-15-8-1 model is the best BPNN model, with a Pearson's correlation coefficient (R) of 0.99507. When milling EN24 on a CNC lathe, Dipti Das et al. [22] investigated surface roughness, regression modelling, and parametric optimization in the context of hard turning. High correlation coefficients R^2 is 0.993 and 0.934 for R_a and R_z , respectively) are found in the prediction models. For both the R_a and R_z surface roughness characteristics, feed is thought to be the most important factor. Arkadeb Mukhopadhyay et al. [23] employed GA and ANN to link surface attributes in wire EDM. Levenberg-Marquardt (L-M) backpropagation was used to train an architecture for a feed-forward ANN. With an overall R^2 value of 0.97, the 4-3-3-1 neural network design has been shown to be capable of quite accurately predicting the fractal dimension. The respective R^2 values for testing, validation, and training are 0.9, 0.99, and 0.99. The model's total R^2 -value is 0.97.

According to the literature review discussed in the paragraphs above, numerous researchers have used ANN models to estimate average roughness, or R_a , with success. Further roughness parameters, such as R_q , R_z , R_p , and R_v , are also necessary to completely evaluate the functional performance of dies (Table 2). This puts particular emphasis on the current approach. This paper presents a method for creating an ANN-based model to predict roughness parameters, including R_z , R_p , R_a , R_q , and R_v , for a thorough functional assessment of Dies manufactured of EN8 steel that has been EDM machined.

3. Materials and methods

3.1. Specimen preparation

ECOLINE ZNC EDM setup was used in this study to perform the experiments. The Dies made from EN8 material are selected for the experimental investigation. The 99% copper electrode of size 1cm x 1cm is used while preparing the dies. Very few experiments are needed, according to the central composite design of the experiment, to forecast optimal conditions among the levels and assigned parameters. It is discovered that the Taguchi L27 array is appropriate for this experimental method of research. The best outcome is produced using 27 trials needed to identify the set of parameter values. The impacts of process parameters are observed through the use of Analysis of Variance (ANOVA). Specimens(Dies) are prepared by changing parameters while an EDM machining process is being performed. Peak Voltage is maintained constant in Table 3 whereas I_p , T_{on} , and T_{off} are variables.

3.2. Measurement of surface roughness

The specimen SR is made with different process parameters that are measured (Table 11) using a profilometer of the Mitsubishi model SJ-410 as shown in Figure 2. Sets of observations are obtained, and the average values are computed for R_a , R_q , R_z , R_p , and R_v .

Table 3.: Input parameters

| Input factors | | Levels | | |
|----------------|-------------------|--------|----|----|
| | Code Units | -1 | 0 | 1 |
| Pulse on time | T_{on} μs | 3 | 5 | 7 |
| Pulse off time | T_{off} μs | 2 | 4 | 6 |
| Peak Current | I_p Amp | 10 | 20 | 30 |

Table 4.: Chemical Composition of EN8 Steel

| Chemical Composition of EN8 Steel | |
|-----------------------------------|------------------|
| Element | Percentage range |
| Carbon | 0.36-0.44 |
| Silicon | 0.05-0.35 |
| Manganese | 0.60-1.00 |
| Phosphorus | 0.015-0.06 |
| Sulphur | 0.015-0.06 |
| Iron | 97.09-98.96 |



Figure 1.: EDM machine - Sparkonix



Figure 2.: Profilometer-SJ410

3.3. Prediction using Response Surface Method (RSM)

Multiple regression is the statistical technique used to predict output parameters. In order to predict roughness parameters R_p , R_v , R_a , R_q , R_z , RSM is used. RSM has been used to build statistical models based on experimental findings. The roughness model in Minitab is created using the response surface approach for surface roughness while accounting for the cutting parameters, which are I_p , T_{Ton} , and T_{off} . By measuring the connections between one or more measured responses and the important input components, RSM makes it easier to examine how the independent factors affect a certain dependent variable (response). In situations when the response function is unknown or non-linear, the second-order equation 1 is usually expressed in the following form.

$$Y = \beta_0 + \sum_{i=1}^k \beta_i \cdot X_i + \sum_{i=1}^k \beta_{ii} \cdot X_i^2 + \sum_{j>1}^k \beta_{ij} \cdot X_i \cdot X_j + \epsilon \quad (1)$$

In this case, the expected result is $(y - \epsilon)$, where ϵ is the noise or error seen in response y and β is the regression coefficient that has to be computed. The least squares method fits a model equation that accounts for the input variables by lowering the residual error, which is calculated by adding the square deviations between the actual and estimated answers. The input variables in this study are denoted by X_i , the squares and interaction terms are denoted by X_i^2 and $X_i \cdot X_j$, respectively, and the related response, or R_a , of the EDM process is denoted by Y . The effects of

EDM parameters T_{on} , T_{off} , and I_p on R_a has been evaluated for EN8 steel. Using the statistical technique of multiple regression, the second-order model was created to determine the relationship between a continuous dependent variable and two or more continuous or discrete independent variables.

3.4. Development of model using Artificial Neural Network (ANN)

Table 5.: Network model parameters

| Parameters | Details | | |
|-----------------------------|---------------------------|----------|---------|
| Network | feed forward net | | |
| Learning rate | 0.01 | | |
| Train,Test,Validation ratio | 0.7, 0.15, 0.15 | | |
| No. of epochs | 300 | | |
| optimizers | trainlm, trainbr, trainrp | | |
| Layer names | Input | Hidden | output |
| Nos. of layers | 3 | 1 | 5 |
| No. of neuorons | 3 | 10 to 15 | 5 |
| Activation function | - | sigmoid | purelin |

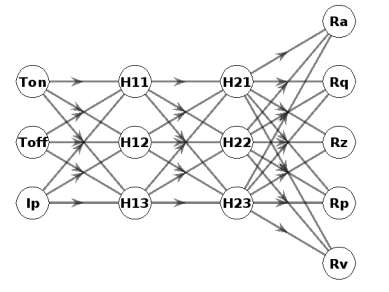


Figure 3.: Neural network diagram

A neural network is composed of several layers, each of which has different neurons. The random noise injection (RNI) technique is used to enrich data in order to improve the model's performance and generalize it more effectively to new data. The type of network depends on its construction. During the learning phase, the network's processing power storage is converted using weights. By changing a network's weights, the training process reduces a chosen function of error between the desired and actual outputs. Input, hidden, and output layers make up its three primary layers. Input layer takes 3 neurons for input variables I_p , T_{on} , and T_{off} . One Hidden layer consists of neurons from 10,11,12,13,14,15. Output layer takes 5 neurons for response variables R_a , R_q , R_z , R_p , R_v . The feedforward net function uses the log-sigmoid (logsig) activation function for the hidden layers and the linear (purelin) activation function for the output layer by default.

Outputs are generated in the hidden layer. The ANN's working is displayed in Figure 3. The model is developed (Figure 4) using MATLAB with three different training algorithms, LM(Levenberg-Marquardt), a classical gradient-based optimization method used to solve non-linear least squares problems. Bayesian Regulation (BR) minimizes a linear combination of squared errors and weights and the detrimental impacts of the partial derivatives magnitudes are eliminated through the use of resilient backpropagation, or RProp. They are used to select the best of these algorithms. Artificial Neural Networks (ANNs) are being trained by the authors to analyze and characterize the topology of a surface using the current methodology. The objective is to develop a method that can accurately assess surface topology using ANNs.

Backpropagation (BP) neural networks are feed-forward artificial neural networks that use an error backpropagation algorithm. as seen in picture 3. The input layer, hidden layer, and output layer comprise the three layers that make up the structure of backpropagation neural networks. The inter-layer transfer function's fundamental idea is that the input vector passes through both the output and hidden layers. The neuron's output value is returned if the demand is not satisfied. By altering the threshold value and connection weight, the learning process is changed. The procedure keeps going until the result value satisfies the specifications and is finished.

The following metrics, defined by equations (2), (3) and (4), will be used for testing the efficacy of the prediction model.

Mean Squared Error (MSE)

$$\text{MSE} = \frac{1}{N} \sum_i |t_i - o_i|^2 \quad (2)$$

Mean Absolute Percentage Error (MAPE)

$$\text{MAPE} = \frac{1}{N} \sum_i \left| \frac{t_i - o_i}{t_i} \right| \times 100 \quad (3)$$

R-squared (R^2)

$$R^2 = 1 - \frac{\sum_i (t_i - o_i)^2}{\sum_i (o_i - \bar{t}_i)^2} \quad (4)$$

where N is the number of experiments, o is the output , \bar{t}_i is the mean value, and t is the target value.

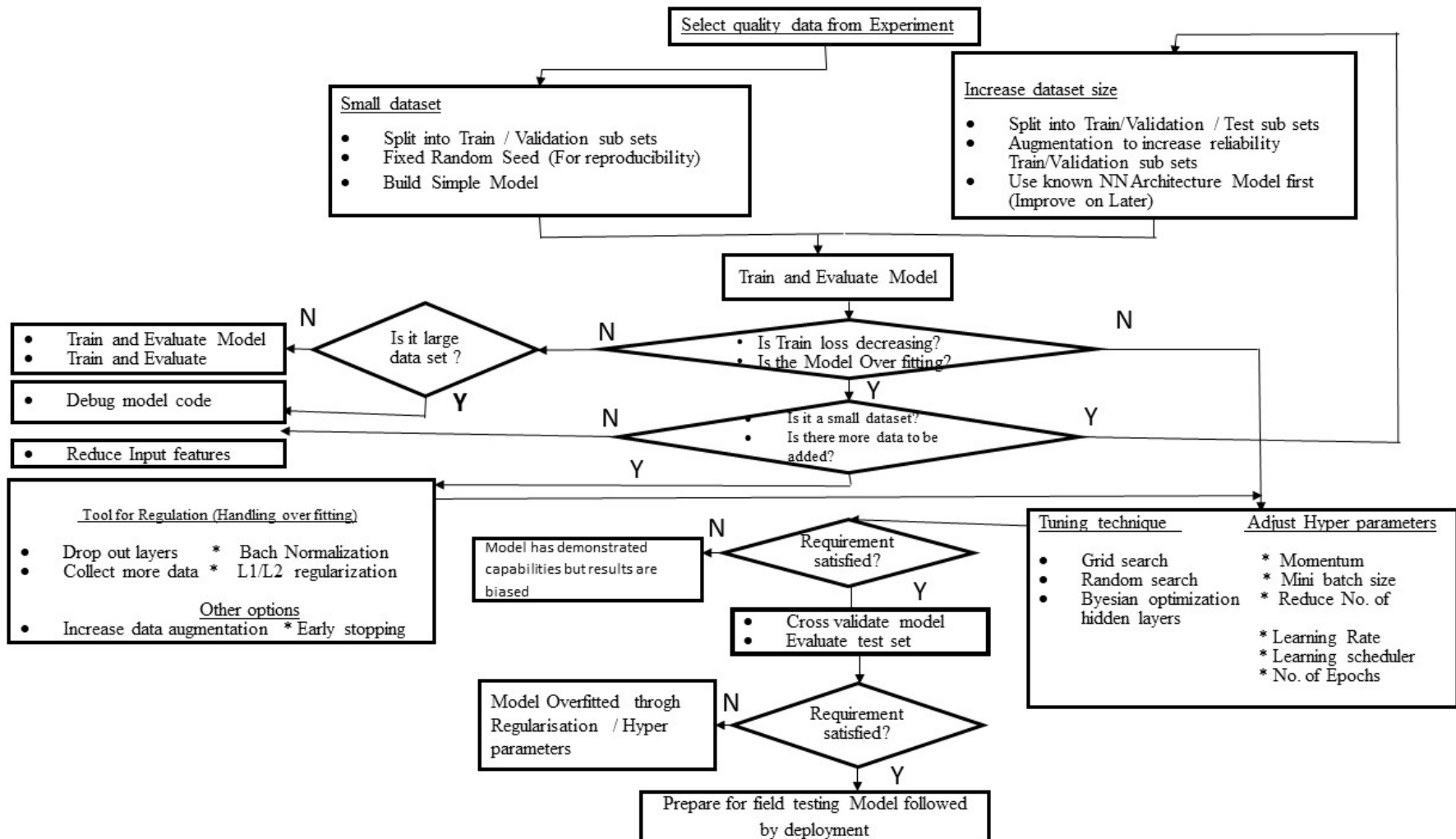


Figure 4.: Flow chart of Artificial Neural Network process

4. Results and discussion

4.1. Analysis of Variance (ANOVA) results

ANOVA technique helps in identifying the most influencing factor affecting the output parameter. The technique uses the sum of squares and variance during analysis. The surface roughness parameters are predicted using input values of T_{on} , T_{off} , I_p . An ANOVA is used to calculate the F-ratio, which is the ratio of the mean square error to the regression mean square. The threshold value of 5% is used to calculate F-0.05. When the calculated F-ratio exceeds F-0.05, the outcome is deemed statistically significant.

Table 6.: ANOVA - Ra

| Source | DF | Adj SS | Adj MS | F-Value | F-0.05 | P-Value |
|-------------------|----|---------|---------|---------|--------|---------|
| Model | 9 | 6.63904 | 0.73767 | 10.59 | 2.49 | 0.000 |
| Linear | 3 | 4.75123 | 1.58374 | 22.73 | 3.20 | 0.000 |
| Ton | 1 | 0.04176 | 0.04176 | 0.6 | 4.45 | 0.449 |
| Toff | 1 | 0.43556 | 0.43556 | 6.25 | 4.45 | 0.023 |
| Ip | 1 | 4.27391 | 4.27391 | 61.34 | 4.45 | 0.000 |
| Square | 3 | 1.21507 | 0.40502 | 5.81 | 3.20 | 0.006 |
| Ton*Ton | 1 | 0.89218 | 0.89218 | 12.8 | 4.45 | 0.002 |
| Toff*Toff | 1 | 0.01357 | 0.01357 | 0.19 | 4.45 | 0.665 |
| Ip*Ip | 1 | 0.30933 | 0.30933 | 4.44 | 4.45 | 0.050 |
| 2-Way Interaction | 3 | 0.67274 | 0.22425 | 3.22 | 3.20 | 0.049 |
| Ton*Toff | 1 | 0.67071 | 0.67071 | 9.63 | 4.45 | 0.006 |
| Ton*Ip | 1 | 0.00066 | 0.00066 | 0.01 | 4.45 | 0.924 |
| Toff*Ip | 1 | 0.00137 | 0.00137 | 0.02 | 4.45 | 0.890 |
| Error | 17 | 1.18447 | 0.06967 | | | |
| Total | 26 | 7.82351 | | | | |

$$\begin{aligned}
 R_a = & 3.27 + 0.744 \cdot T_{on} - 0.302 \cdot T_{off} - 0.0418 \cdot I_p \\
 & - 0.0964 \cdot T_{on}^2 + 0.0119 \cdot T_{off}^2 + 0.00227 \cdot I_p^2 \\
 & + 0.0591 \cdot T_{on} \cdot T_{off} + 0.00037 \cdot T_{on} \cdot I_p - 0.00053 \cdot T_{off} \cdot I_p
 \end{aligned} \tag{5a}$$

Table 8.: ANOVA - Rz

| Source | DF | Adj SS | Adj MS | F-Value | F-0.05 | P-Value |
|-------------------|----|---------|---------|---------|--------|---------|
| Model | 9 | 113.408 | 12.6009 | 3.31 | 2.49 | 0.016 |
| Linear | 3 | 38.59 | 12.8633 | 3.38 | 3.2 | 0.043 |
| Ton | 1 | 0.56 | 0.5597 | 0.15 | 4.45 | 0.706 |
| Toff | 1 | 0.858 | 0.8581 | 0.23 | 4.45 | 0.641 |
| Ip | 1 | 37.172 | 37.1723 | 9.76 | 4.45 | 0.006 |
| Square | 3 | 39.498 | 13.1659 | 3.46 | 3.2 | 0.04 |
| Ton*Ton | 1 | 31.94 | 31.9396 | 8.38 | 4.45 | 0.01 |
| Toff*Toff | 1 | 5.179 | 5.1795 | 1.36 | 4.45 | 0.26 |
| Ip*Ip | 1 | 2.378 | 2.3785 | 0.62 | 4.45 | 0.44 |
| 2-Way Interaction | 3 | 35.32 | 11.7735 | 3.09 | 3.2 | 0.055 |
| Ton*Toff | 1 | 30.694 | 30.6944 | 8.06 | 4.45 | 0.011 |
| Ton*Ip | 1 | 0.157 | 0.1571 | 0.04 | 4.45 | 0.841 |
| Toff*Ip | 1 | 4.469 | 4.4689 | 1.17 | 4.45 | 0.294 |
| Error | 17 | 64.768 | 3.8099 | | | |
| Total | 26 | 178.176 | | | | |

$$\begin{aligned}
 R_z = & 28.07 + 3.97 \cdot T_{on} - 4.58 \cdot T_{off} - 0.259 \cdot I_p \\
 & - 0.577 \cdot T_{on}^2 + 0.232 \cdot T_{off}^2 + 0.00630 \cdot I_p^2 \\
 & + 0.400 \cdot T_{on} \cdot T_{off} + 0.0057 \cdot T_{on} \cdot I_p + 0.0305 \cdot T_{off} \cdot I_p
 \end{aligned} \tag{5c}$$

Table 7.: ANOVA - Rq

| Source | DF | Adj SS | Adj MS | F-Value | F-0.05 | P-Value |
|-------------------|----|---------|---------|---------|--------|---------|
| Model | 9 | 9.9123 | 1.10136 | 7.37 | 2.49 | 0 |
| Linear | 3 | 6.027 | 2.009 | 13.45 | 3.2 | 0 |
| Ton | 1 | 0.0009 | 0.00087 | 0.01 | 4.45 | 0.94 |
| Toff | 1 | 0.1961 | 0.19615 | 1.31 | 4.45 | 0.268 |
| Ip | 1 | 5.83 | 5.82997 | 39.04 | 4.45 | 0 |
| Square | 3 | 2.7048 | 0.90161 | 6.04 | 3.2 | 0.005 |
| Ton*Ton | 1 | 2.1877 | 2.18769 | 14.65 | 4.45 | 0.001 |
| Toff*Toff | 1 | 0.1501 | 0.1501 | 1.01 | 4.45 | 0.33 |
| Ip*Ip | 1 | 0.367 | 0.36704 | 2.46 | 4.45 | 0.135 |
| 2-Way Interaction | 3 | 1.1805 | 0.39349 | 2.63 | 3.2 | 0.083 |
| Ton*Toff | 1 | 1.139 | 1.13898 | 7.63 | 4.45 | 0.013 |
| Ton*Ip | 1 | 0.0137 | 0.01374 | 0.09 | 4.45 | 0.765 |
| Toff*Ip | 1 | 0.0277 | 0.02774 | 0.19 | 4.45 | 0.672 |
| Error | 17 | 2.539 | 0.14935 | | | |
| Total | 26 | 12.4512 | | | | |

$$\begin{aligned}
 R_q = & 4.13 + 1.239 \cdot T_{on} - 0.697 \cdot T_{off} - 0.0432 \cdot I_p \\
 & - 0.1510 \cdot T_{on}^2 + 0.0395 \cdot T_{off}^2 + 0.00247 \cdot I_p^2 \\
 & + 0.0770 \cdot T_{on} \cdot T_{off} - 0.00169 \cdot T_{on} \cdot I_p + 0.00240 \cdot T_{off} \cdot I_p
 \end{aligned} \tag{5b}$$

Table 9.: ANOVA - Rp

| Source | DF | Adj SS | Adj MS | F-Value | F-0.05 | P-Value |
|-------------------|----|---------|---------|---------|--------|---------|
| Model | 9 | 40.874 | 4.5416 | 1.03 | 2.49 | 0.453 |
| Linear | 3 | 17.638 | 5.8793 | 1.34 | 3.2 | 0.295 |
| Ton | 1 | 0.003 | 0.0028 | 0 | 4.45 | 0.98 |
| Toff | 1 | 1.491 | 1.4907 | 0.34 | 4.45 | 0.568 |
| Ip | 1 | 16.144 | 16.1445 | 3.68 | 4.45 | 0.072 |
| Square | 3 | 19.111 | 6.3702 | 1.45 | 3.2 | 0.263 |
| Ton*Ton | 1 | 10.738 | 10.7379 | 2.45 | 4.45 | 0.136 |
| Toff*Toff | 1 | 6.967 | 6.9668 | 1.59 | 4.45 | 0.225 |
| Ip*Ip | 1 | 1.406 | 1.4059 | 0.32 | 4.45 | 0.579 |
| 2-Way Interaction | 3 | 4.126 | 1.3753 | 0.31 | 3.2 | 0.816 |
| Ton*Toff | 1 | 0.736 | 0.7356 | 0.17 | 4.45 | 0.687 |
| Ton*Ip | 1 | 1.064 | 1.0645 | 0.24 | 4.45 | 0.629 |
| Toff*Ip | 1 | 2.326 | 2.3258 | 0.53 | 4.45 | 0.477 |
| Error | 17 | 74.639 | 4.3905 | | | |
| Total | 26 | 115.513 | | | | |

$$\begin{aligned}
 R_p = & 9.80 + 3.40 \cdot T_{on} - 3.05 \cdot T_{off} - 0.113 \cdot I_p \\
 & - 0.334 \cdot T_{on}^2 + 0.269 \cdot T_{off}^2 + 0.00484 \cdot I_p^2
 \end{aligned} \tag{5d}$$

Table 10.: ANOVA - Rv

| Source | DF | Adj SS | Adj MS | F-Value | F-0.05 | P-Value |
|-------------------|----|---------|--------|---------|--------|---------|
| Model | 9 | 35.7452 | 3.9717 | 3.46 | 2.49 | 0.013 |
| Linear | 3 | 4.7257 | 1.5752 | 1.37 | 3.2 | 0.285 |
| Ton | 1 | 0.3192 | 0.3192 | 0.28 | 4.45 | 0.605 |
| Toff | 1 | 0.0867 | 0.0867 | 0.08 | 4.45 | 0.787 |
| Ip | 1 | 4.3198 | 4.3198 | 3.77 | 4.45 | 0.069 |
| Square | 3 | 6.7084 | 2.2361 | 1.95 | 3.2 | 0.16 |
| Ton*Ton | 1 | 6.3044 | 6.3044 | 5.49 | 4.45 | 0.031 |
| Toff*Toff | 1 | 0.0084 | 0.0084 | 0.01 | 4.45 | 0.933 |
| Ip*Ip | 1 | 0.3956 | 0.3956 | 0.34 | 4.45 | 0.565 |
| 2-Way Interaction | 3 | 24.3111 | 8.1037 | 7.06 | 3.2 | 0.003 |
| Ton*Toff | 1 | 21.924 | 21.924 | 19.11 | 4.45 | 0 |
| Ton*Ip | 1 | 2.0402 | 2.0402 | 1.78 | 4.45 | 0.2 |
| Toff*Ip | 1 | 0.3468 | 0.3468 | 0.3 | 4.45 | 0.59 |
| Error | 17 | 19.5052 | 1.1474 | | | |
| Total | 26 | 55.2503 | | | | |

$$\begin{aligned}
 R_v = & 19.45 + 1.48 \cdot T_{on} - 2.348 \cdot T_{off} - 0.310 \cdot I_p \\
 & - 0.331 \cdot T_{on}^2 + 0.0280 \cdot T_{off}^2 + 0.00406 \cdot I_p^2 \\
 & + 0.3379 \cdot T_{on} \cdot T_{off} + 0.0206 \cdot T_{on} \cdot I_p + 0.0197 \cdot T_{off} \cdot I_p
 \end{aligned} \quad (5e)$$

Figure 5 shows a line chart comparison of actual and predicted values of R_a , R_q , R_z , R_p , R_v . It can be seen that both the actual and predicted values are in proximity, showing the strength of the RSM model.

The results of the experiment (Table 11) show that the main variables affecting the SR of EN8 material during EDM machining are the discharge current (I_p), pulse-on time (T_{on}), and pulse-off time (T_{off}). Pulse-on time is found to be the main factor influencing surface roughness. It was also observed that surface roughness increased when I_p rose. The confirmation test results showed that the developed models have a 95% confidence interval for correctly predicting the SR (Table 12). The optimization process is established by the selected approach, which makes it easier to use EDM machinable EN8 in industrial applications.

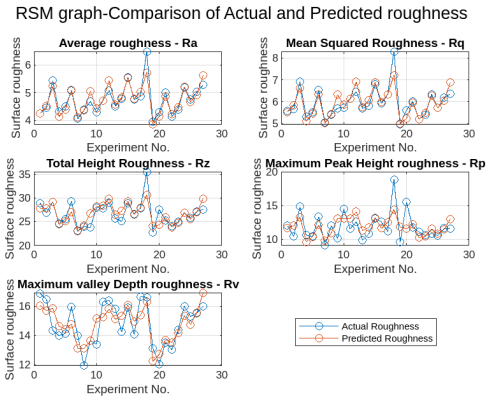


Figure 5.: RSM - comparison plots

4.2. Result analysis using ANOVA

Table 11.: RSM - Experiment and predicted Results

| Exp | Input factors | | | | Experiment Output variables | | | | | Predicted Output variables | | | | |
|-----|---------------|-----------------|------------------|----------------|-----------------------------|----------------|----------------|----------------|----------------|----------------------------|----------------|----------------|----------------|----------------|
| | No | T _{on} | T _{off} | I _p | R _a | R _q | R _z | R _p | R _v | R _a | R _q | R _z | R _p | R _v |
| 1 | 3 | 2 | 10 | 4.252 | 5.585 | 28.935 | 12.071 | 16.865 | 4.247 | 5.527 | 27.77 | 11.7 | 16.042 | |
| 2 | 3 | 2 | 20 | 4.442 | 5.664 | 26.886 | 10.423 | 16.462 | 4.511 | 5.834 | 27.86 | 12.02 | 15.693 | |
| 3 | 3 | 2 | 30 | 5.428 | 6.928 | 29.213 | 14.856 | 14.356 | 5.228 | 6.636 | 29.2 | 13.3 | 15.857 | |
| 4 | 3 | 4 | 10 | 4.317 | 5.309 | 24.604 | 10.612 | 13.992 | 4.13 | 5.117 | 24.42 | 9.64 | 14.627 | |
| 5 | 3 | 4 | 20 | 4.489 | 5.518 | 25.57 | 10.429 | 14.141 | 4.382 | 5.472 | 25.11 | 10.4 | 14.448 | |
| 6 | 3 | 4 | 30 | 5.061 | 6.529 | 29.292 | 13.338 | 15.954 | 5.089 | 6.323 | 27.06 | 12.13 | 14.783 | |
| 7 | 3 | 6 | 10 | 4.047 | 5.047 | 23.099 | 9.117 | 13.982 | 4.107 | 5.023 | 22.92 | 9.74 | 13.138 | |
| 8 | 3 | 6 | 20 | 4.372 | 5.399 | 23.959 | 12.019 | 11.94 | 4.349 | 5.427 | 24.22 | 10.95 | 13.129 | |
| 9 | 3 | 6 | 30 | 4.681 | 5.705 | 23.789 | 10.131 | 13.658 | 5.045 | 6.325 | 26.78 | 13.11 | 13.633 | |
| 10 | 5 | 2 | 10 | 4.296 | 5.735 | 27.909 | 14.507 | 13.402 | 4.437 | 5.863 | 28.19 | 13.1 | 15.17 | |
| 11 | 5 | 2 | 20 | 4.706 | 6.136 | 27.858 | 11.558 | 16.3 | 4.708 | 6.137 | 28.39 | 13.12 | 15.233 | |
| 12 | 5 | 2 | 30 | 5.077 | 6.45 | 29.005 | 12.618 | 16.388 | 5.433 | 6.905 | 29.85 | 14.11 | 15.81 | |
| 13 | 5 | 4 | 10 | 4.506 | 5.695 | 25.707 | 9.887 | 15.82 | 4.556 | 5.761 | 26.43 | 11.29 | 15.107 | |
| 14 | 5 | 4 | 20 | 4.761 | 5.803 | 25.066 | 10.824 | 14.242 | 4.816 | 6.083 | 27.24 | 11.75 | 15.34 | |
| 15 | 5 | 4 | 30 | 5.561 | 6.807 | 28.956 | 13.056 | 15.9 | 5.53 | 6.9 | 29.31 | 13.18 | 16.087 | |
| 16 | 5 | 6 | 10 | 4.742 | 5.915 | 26.665 | 12.601 | 14.064 | 4.77 | 5.976 | 26.53 | 11.64 | 14.969 | |
| 17 | 5 | 6 | 20 | 4.864 | 6.344 | 27.857 | 11.205 | 16.651 | 5.019 | 6.346 | 27.95 | 12.54 | 15.372 | |
| 18 | 5 | 6 | 30 | 6.48 | 8.296 | 35.502 | 18.892 | 16.61 | 5.723 | 7.21 | 30.63 | 14.41 | 16.289 | |
| 19 | 7 | 2 | 10 | 3.936 | 4.971 | 22.736 | 9.606 | 13.13 | 3.856 | 4.992 | 23.99 | 11.82 | 12.248 | |
| 20 | 7 | 2 | 20 | 4.278 | 5.611 | 27.583 | 15.535 | 12.048 | 4.134 | 5.232 | 24.31 | 11.55 | 12.723 | |
| 21 | 7 | 2 | 30 | 5.007 | 6.013 | 25.309 | 11.77 | 13.539 | 4.867 | 5.966 | 25.88 | 12.24 | 13.712 | |
| 22 | 7 | 4 | 10 | 4.133 | 5.202 | 24.117 | 11.084 | 13.033 | 4.211 | 5.198 | 23.84 | 10.26 | 13.536 | |
| 23 | 7 | 4 | 20 | 4.389 | 5.409 | 24.965 | 10.593 | 14.372 | 4.479 | 5.486 | 24.76 | 10.43 | 14.182 | |
| 24 | 7 | 4 | 30 | 5.177 | 6.337 | 26.83 | 10.833 | 15.997 | 5.2 | 6.269 | 26.94 | 11.56 | 15.341 | |
| 25 | 7 | 6 | 10 | 4.746 | 5.719 | 25.865 | 10.565 | 15.3 | 4.661 | 5.721 | 25.54 | 10.86 | 14.75 | |
| 26 | 7 | 6 | 20 | 5.016 | 6.19 | 27.16 | 11.631 | 15.53 | 4.918 | 6.057 | 27.07 | 11.47 | 15.566 | |
| 27 | 7 | 6 | 30 | 5.274 | 6.357 | 27.608 | 11.603 | 16.004 | 5.629 | 6.888 | 29.86 | 13.04 | 16.895 | |

Summarised Results of RSM method are given in Table 12 for MSE, MAPE and R².

Table 12.: MSE, MAPE and R² values for RSM

| Metrics | Surface roughness values | | | | |
|----------------|--------------------------|----------------|----------------|----------------|----------------|
| | Roughness | R _a | R _q | R _z | R _p |
| MSE | 0.043847 | 0.094043 | 2.397050 | 2.763526 | 0.722331 |
| MAPE | 2.743692 | 2.948027 | 3.598553 | 10.349331 | 5.007920 |
| R ² | 0.998075 | 0.997379 | 0.996679 | 0.981065 | 0.996734 |

4.3. ANN result discussion

The system is modelled using machine learning which produced very low MAPE, MSE, and high R². Several models were put forth in this study, and their respective performances were compared. Fundamentally, three distinct approaches were employed: LM optimizer, BR, and Rprop. The three approaches differ mostly in terms of training duration and effectiveness. The dataset typically determines how well the techniques train.

4.4. Artificial Neural Network (ANN) results

Table 13.: ANN results of BR optimizer for training, validation and testing

| Architecture | TRAINING RESULTS - BR | | | | | | | | | | | | | | |
|--------------------|-----------------------|----------------|----------------|----------------|----------------|----------------|----------------|----------------|----------------|----------------|----------------|----------------|----------------|----------------|----------|
| | MSE | | | | | MAPE | | | | | R2 | | | | |
| R _a | R _q | R _z | R _p | R _v | R _a | R _q | R _z | R _p | R _v | R _a | R _q | R _z | R _p | R _v | |
| 3,10,5 | 0.008671 | 0.010092 | 0.007071 | 0.006650 | 0.005111 | 1.360240 | 1.263457 | 0.211768 | 0.440678 | 0.304238 | 0.971957 | 0.980354 | 0.999017 | 0.998588 | 0.997482 |
| 3,11,5 | 0.002044 | 0.004412 | 0.002985 | 0.003315 | 0.002239 | 0.743530 | 0.831575 | 0.152446 | 0.362269 | 0.251347 | 0.993390 | 0.991411 | 0.999585 | 0.999296 | 0.998897 |
| 3,12,5 | 0.001578 | 0.000610 | 0.001714 | 0.001880 | 0.001662 | 0.719659 | 0.350167 | 0.121803 | 0.286908 | 0.204912 | 0.994897 | 0.998813 | 0.999762 | 0.999601 | 0.999181 |
| 3,13,5 | 0.000891 | 0.001225 | 0.001729 | 0.002061 | 0.001662 | 0.496790 | 0.464177 | 0.123589 | 0.304240 | 0.207499 | 0.997118 | 0.997615 | 0.999759 | 0.999562 | 0.999181 |
| 3,14,5 | 0.000380 | 0.000439 | 0.000967 | 0.000764 | 0.000401 | 0.329527 | 0.285457 | 0.084431 | 0.162843 | 0.107313 | 0.998770 | 0.999145 | 0.999866 | 0.999838 | 0.999802 |
| 3,15,5 | 0.000230 | 0.000267 | 0.000809 | 0.000660 | 0.000373 | 0.244474 | 0.220594 | 0.079221 | 0.160696 | 0.102858 | 0.999257 | 0.999481 | 0.999887 | 0.999860 | 0.999816 |
| VALIDATION RESULTS | | | | | | | | | | | | | | | |
| 3,10,5 | 0.011812 | 0.010935 | 0.005346 | 0.005116 | 0.003454 | 1.605832 | 1.291755 | 0.208549 | 0.408273 | 0.264865 | 0.944430 | 0.967696 | 0.998889 | 0.998552 | 0.997753 |
| 3,11,5 | 0.002609 | 0.004742 | 0.002688 | 0.002802 | 0.001829 | 0.885122 | 0.930550 | 0.149757 | 0.310524 | 0.217438 | 0.987728 | 0.985991 | 0.999441 | 0.999207 | 0.998810 |
| 3,12,5 | 0.001715 | 0.000584 | 0.002105 | 0.001660 | 0.001822 | 0.749121 | 0.336067 | 0.141351 | 0.259912 | 0.215168 | 0.991934 | 0.998275 | 0.999562 | 0.999530 | 0.998815 |
| 3,13,5 | 0.000888 | 0.001207 | 0.001634 | 0.002252 | 0.001735 | 0.494760 | 0.491064 | 0.119229 | 0.326955 | 0.209087 | 0.995824 | 0.996433 | 0.999660 | 0.999363 | 0.998871 |
| 3,14,5 | 0.000403 | 0.000431 | 0.001100 | 0.000823 | 0.000409 | 0.317149 | 0.286867 | 0.086125 | 0.165375 | 0.107832 | 0.998104 | 0.998727 | 0.999771 | 0.999767 | 0.999734 |
| 3,15,5 | 0.000279 | 0.000208 | 0.000760 | 0.000651 | 0.000371 | 0.259022 | 0.194200 | 0.077171 | 0.164769 | 0.095526 | 0.998687 | 0.999387 | 0.999842 | 0.999816 | 0.999758 |
| TESTING RESULTS | | | | | | | | | | | | | | | |
| 3,10,5 | 0.009537 | 0.012052 | 0.009087 | 0.011724 | 0.006972 | 1.377630 | 1.388836 | 0.233991 | 0.519499 | 0.353514 | 0.968008 | 0.975543 | 0.998639 | 0.997652 | 0.996423 |
| 3,11,5 | 0.002138 | 0.005081 | 0.002959 | 0.004980 | 0.002827 | 0.745567 | 0.913703 | 0.153382 | 0.428707 | 0.278407 | 0.992828 | 0.989690 | 0.999557 | 0.999003 | 0.998549 |
| 3,12,5 | 0.001575 | 0.000535 | 0.002215 | 0.002132 | 0.001754 | 0.711073 | 0.314445 | 0.134448 | 0.294705 | 0.209037 | 0.994716 | 0.998915 | 0.999668 | 0.999573 | 0.999100 |
| 3,13,5 | 0.000918 | 0.001250 | 0.001631 | 0.001967 | 0.001683 | 0.485867 | 0.459264 | 0.117219 | 0.297136 | 0.207335 | 0.996920 | 0.997464 | 0.999756 | 0.999606 | 0.999136 |
| 3,14,5 | 0.000358 | 0.000473 | 0.001234 | 0.001384 | 0.000397 | 0.304171 | 0.292979 | 0.091349 | 0.198505 | 0.102452 | 0.998798 | 0.999040 | 0.999815 | 0.999723 | 0.999796 |
| 3,15,5 | 0.000210 | 0.000225 | 0.000662 | 0.000726 | 0.000326 | 0.221067 | 0.196572 | 0.073058 | 0.182743 | 0.097035 | 0.999297 | 0.999543 | 0.999901 | 0.999855 | 0.999833 |

Table 14.: Summary results of BR optimizer

| Optimizer | Result Summary-BR | | | | | | | | | | | | | | |
|------------------------|-------------------|----------------|----------------|----------------|----------------|----------------|----------------|----------------|----------------|----------------|----------------|----------------|----------------|----------------|----------------|
| | MSE-MINIMUM | | | | | MAPE-MINIMUM | | | | | R2-MAXIMUM | | | | |
| Process (Architecture) | R _a | R _q | R _z | R _p | R _v | R _a | R _q | R _z | R _p | R _v | R _a | R _q | R _z | R _p | R _v |
| TRAINING (3,15,5) | 0.00023 | 0.00027 | 0.00081 | 0.00066 | 0.00037 | 0.24447 | 0.22059 | 0.07922 | 0.16070 | 0.10286 | 0.99926 | 0.99948 | 0.99989 | 0.99986 | 0.99982 |
| VALIDATION (3,15,5) | 0.00028 | 0.00021 | 0.00076 | 0.00065 | 0.00037 | 0.25902 | 0.19420 | 0.07717 | 0.16477 | 0.09553 | 0.99869 | 0.99939 | 0.99984 | 0.99982 | 0.99976 |
| TESTING (3,15,5) | 0.00021 | 0.00023 | 0.00066 | 0.00073 | 0.00033 | 0.22107 | 0.19657 | 0.07306 | 0.18274 | 0.09703 | 0.99930 | 0.99954 | 0.99990 | 0.99985 | 0.99983 |

Table 13 shows performance measures, MSE, MAPE, and R², as well as the outcomes of the BR optimizer when forecasting the surface parameters R_a, R_q, R_z, R_p, and R_v following the training of an ANN model using input data Ton, Toff, and I_p. Each row displays architecture values between 3,10,5, and 3,15,5. The first digit 3 indicates the number of neurons in the input layers. The middle digits 10 and 15, indicate the number of neurons in a hidden layer. The third numeral 5 indicates the number of neurons in the output layer. Table 14 shows lowest MSE and MAPE values and the highest R² value for testing, validation, and training using the best architecture (3,15,5).

Table 15.: ANN results of LM optimizer for training, validation, and testing

| | TRAINING RESULTS - LM | | | | | | | | | | | | | | |
|--------------|-----------------------|----------------|----------------|----------------|----------------|----------------|----------------|----------------|----------------|----------------|----------------|----------------|----------------|----------------|----------------|
| | MSE | | | | | MAPE | | | | | R2 | | | | |
| Architecture | R _a | R _q | R _z | R _p | R _v | R _a | R _q | R _z | R _p | R _v | R _a | R _q | R _z | R _p | R _v |
| 3,10,5 | 0.008671 | 0.010092 | 0.007071 | 0.006650 | 0.005111 | 1.360240 | 1.263457 | 0.211768 | 0.440678 | 0.304238 | 0.971957 | 0.980354 | 0.999017 | 0.998588 | 0.997482 |
| 3,11,5 | 0.002044 | 0.004412 | 0.002985 | 0.003315 | 0.002239 | 0.743530 | 0.831575 | 0.152446 | 0.362269 | 0.251347 | 0.993390 | 0.991411 | 0.999585 | 0.999296 | 0.998897 |
| 3,12,5 | 0.001578 | 0.000610 | 0.001714 | 0.001880 | 0.001662 | 0.719659 | 0.350167 | 0.121803 | 0.286908 | 0.204912 | 0.994897 | 0.998813 | 0.999762 | 0.999601 | 0.999181 |
| 3,13,5 | 0.000891 | 0.001225 | 0.001729 | 0.002061 | 0.001662 | 0.496790 | 0.464177 | 0.123589 | 0.304240 | 0.207499 | 0.997118 | 0.997615 | 0.999759 | 0.999562 | 0.999181 |
| 3,14,5 | 0.000380 | 0.000439 | 0.000967 | 0.000764 | 0.000401 | 0.329527 | 0.285457 | 0.084431 | 0.162843 | 0.107313 | 0.998770 | 0.999145 | 0.999866 | 0.999838 | 0.999802 |
| 3,15,5 | 0.000230 | 0.000267 | 0.000809 | 0.000660 | 0.000373 | 0.244474 | 0.220594 | 0.079221 | 0.160696 | 0.102858 | 0.999257 | 0.999481 | 0.999887 | 0.999860 | 0.999816 |
| | VALIDATION RESULTS | | | | | | | | | | | | | | |
| 3,10,5 | 0.011812 | 0.010935 | 0.005346 | 0.005116 | 0.003454 | 1.605832 | 1.291755 | 0.208549 | 0.408273 | 0.264865 | 0.944430 | 0.967696 | 0.998889 | 0.998552 | 0.997753 |
| 3,11,5 | 0.002609 | 0.004742 | 0.002688 | 0.002802 | 0.001829 | 0.885122 | 0.930550 | 0.149757 | 0.310524 | 0.217438 | 0.987728 | 0.985991 | 0.999441 | 0.999207 | 0.998810 |
| 3,12,5 | 0.001715 | 0.000584 | 0.002105 | 0.001660 | 0.001822 | 0.749121 | 0.336067 | 0.141351 | 0.259912 | 0.215168 | 0.991934 | 0.998275 | 0.999562 | 0.999530 | 0.998815 |
| 3,13,5 | 0.000888 | 0.001207 | 0.001634 | 0.002252 | 0.001735 | 0.494760 | 0.491064 | 0.119229 | 0.326955 | 0.209087 | 0.995824 | 0.996433 | 0.999660 | 0.999363 | 0.998871 |
| 3,14,5 | 0.000403 | 0.000431 | 0.001100 | 0.000823 | 0.000409 | 0.317149 | 0.286867 | 0.086125 | 0.165375 | 0.107832 | 0.998104 | 0.998727 | 0.999771 | 0.999767 | 0.999734 |
| 3,15,5 | 0.000279 | 0.000208 | 0.000760 | 0.000651 | 0.000371 | 0.259022 | 0.194200 | 0.077171 | 0.164769 | 0.095526 | 0.998687 | 0.999387 | 0.999842 | 0.999816 | 0.999758 |
| | TESTING RESULTS | | | | | | | | | | | | | | |
| 3,10,5 | 0.009537 | 0.012052 | 0.009087 | 0.011724 | 0.006972 | 1.377630 | 1.388836 | 0.233991 | 0.519499 | 0.353514 | 0.968008 | 0.975543 | 0.998639 | 0.997652 | 0.996423 |
| 3,11,5 | 0.002138 | 0.005081 | 0.002959 | 0.004980 | 0.002827 | 0.745567 | 0.913703 | 0.153382 | 0.428707 | 0.278407 | 0.992828 | 0.989690 | 0.999557 | 0.999003 | 0.998549 |
| 3,12,5 | 0.001575 | 0.000535 | 0.002215 | 0.002132 | 0.001754 | 0.711073 | 0.314445 | 0.134448 | 0.294705 | 0.209037 | 0.994716 | 0.998915 | 0.999668 | 0.999573 | 0.999100 |
| 3,13,5 | 0.000918 | 0.001250 | 0.001631 | 0.001967 | 0.001683 | 0.485867 | 0.459264 | 0.117219 | 0.297136 | 0.207335 | 0.996920 | 0.997464 | 0.999756 | 0.999606 | 0.999136 |
| 3,14,5 | 0.000358 | 0.000473 | 0.001234 | 0.001384 | 0.000397 | 0.304171 | 0.292979 | 0.091349 | 0.198505 | 0.102452 | 0.998798 | 0.999040 | 0.999815 | 0.999723 | 0.999796 |
| 3,15,5 | 0.000210 | 0.000225 | 0.000662 | 0.000726 | 0.000326 | 0.221067 | 0.196572 | 0.073058 | 0.182743 | 0.097035 | 0.999297 | 0.999543 | 0.999901 | 0.999855 | 0.999833 |

Table 16.: Summary results of LM optimizer

| | Result Summary-LM | | | | | | | | | | | | | | |
|---------------------|-------------------|---------|---------|---------|---------|--------------|---------|---------|---------|---------|------------|---------|---------|---------|---------|
| | MSE-MINIMUM | | | | | MAPE-MINIMUM | | | | | R2-MAXIMUM | | | | |
| TRAINING (3,15,5) | 0.00019 | 0.00019 | 0.00045 | 0.00034 | 0.00035 | 0.22421 | 0.17998 | 0.05936 | 0.11588 | 0.09217 | 0.99938 | 0.99964 | 0.99994 | 0.99993 | 0.99983 |
| VALIDATION (3,15,5) | 0.00025 | 0.00026 | 0.00039 | 0.00034 | 0.00033 | 0.27609 | 0.22148 | 0.05460 | 0.11095 | 0.09190 | 0.99881 | 0.99922 | 0.99992 | 0.99990 | 0.99978 |
| TESTING (3,15,5) | 0.00019 | 0.00022 | 0.00039 | 0.00030 | 0.00041 | 0.22873 | 0.19775 | 0.05561 | 0.11017 | 0.10169 | 0.99936 | 0.99956 | 0.99994 | 0.99994 | 0.99979 |

Table 15 shows performance measures, MSE, MAPE, and R^2 , as well as the outcomes of the LM optimizer when forecasting the surface parameters R_a , R_q , R_z , R_p , and R_v following the training of an ANN model using input data T_{on} , T_{off} , and I_p . Each row displays architecture values between 3,10,5 and 3,15,5. The first digit 3 indicates the number of neurons in the input layers. The middle digit 10 and 15 indicate the number of neurons in a hidden layer. The third numeral 5 indicates the number of neurons in the output layer. Table 16 shows lowest MSE and MAPE values and the highest R^2 value for testing, validation, and training using the best architecture (3,15,5).

Table 17.: ANN results of RProp optimizer for training, validation and testing

| | TRAINING RESULTS - RProp | | | | | | | | | | | | | | |
|--------------|--------------------------|----------------|----------------|----------------|----------------|----------------|----------------|----------------|----------------|----------------|----------------|----------------|----------------|----------------|----------------|
| | MSE | | | | | MAPE | | | | | R2 | | | | |
| Architecture | R _a | R _q | R _z | R _p | R _v | R _a | R _q | R _z | R _p | R _v | R _a | R _q | R _z | R _p | R _v |
| 3,10,5 | 0.008671 | 0.010092 | 0.007071 | 0.006650 | 0.005111 | 1.360240 | 1.263457 | 0.211768 | 0.440678 | 0.304238 | 0.971957 | 0.980354 | 0.999017 | 0.998588 | 0.997482 |
| 3,11,5 | 0.002044 | 0.004412 | 0.002985 | 0.003315 | 0.002239 | 0.743530 | 0.831575 | 0.152446 | 0.362269 | 0.251347 | 0.993390 | 0.991411 | 0.999585 | 0.999296 | 0.998897 |
| 3,12,5 | 0.001578 | 0.000610 | 0.001714 | 0.001880 | 0.001662 | 0.719659 | 0.350167 | 0.121803 | 0.286908 | 0.204912 | 0.994897 | 0.998813 | 0.999762 | 0.999601 | 0.999181 |
| 3,13,5 | 0.000891 | 0.001225 | 0.001729 | 0.002061 | 0.001662 | 0.496790 | 0.464177 | 0.123589 | 0.304240 | 0.207499 | 0.997118 | 0.997615 | 0.999759 | 0.999562 | 0.999181 |
| 3,14,5 | 0.000380 | 0.000439 | 0.000967 | 0.000764 | 0.000401 | 0.329527 | 0.285457 | 0.084431 | 0.162843 | 0.107313 | 0.998770 | 0.999145 | 0.999866 | 0.999838 | 0.999802 |
| 3,15,5 | 0.000230 | 0.000267 | 0.000809 | 0.000660 | 0.000373 | 0.244474 | 0.220594 | 0.079221 | 0.160696 | 0.102858 | 0.999257 | 0.999481 | 0.999887 | 0.999860 | 0.999816 |
| | VALIDATION RESULTS | | | | | | | | | | | | | | |
| 3,10,5 | 0.011812 | 0.010935 | 0.005346 | 0.005116 | 0.003454 | 1.605832 | 1.291755 | 0.208549 | 0.408273 | 0.264865 | 0.944430 | 0.967696 | 0.998889 | 0.998552 | 0.997753 |
| 3,11,5 | 0.002609 | 0.004742 | 0.002688 | 0.002802 | 0.001829 | 0.885122 | 0.930550 | 0.149757 | 0.310524 | 0.217438 | 0.987728 | 0.985991 | 0.999441 | 0.999207 | 0.998810 |
| 3,12,5 | 0.001715 | 0.000584 | 0.002105 | 0.001660 | 0.001822 | 0.749121 | 0.336067 | 0.141351 | 0.259912 | 0.215168 | 0.991934 | 0.998275 | 0.999562 | 0.999530 | 0.998815 |
| 3,13,5 | 0.000888 | 0.001207 | 0.001634 | 0.002252 | 0.001735 | 0.494760 | 0.491064 | 0.119229 | 0.326955 | 0.209087 | 0.995824 | 0.996433 | 0.999660 | 0.999363 | 0.998871 |
| 3,14,5 | 0.000403 | 0.000431 | 0.001100 | 0.000823 | 0.000409 | 0.317149 | 0.286867 | 0.086125 | 0.165375 | 0.107832 | 0.998104 | 0.998727 | 0.999771 | 0.999767 | 0.999734 |
| 3,15,5 | 0.000279 | 0.000208 | 0.000760 | 0.000651 | 0.000371 | 0.259022 | 0.194200 | 0.077171 | 0.164769 | 0.095526 | 0.998687 | 0.999387 | 0.999842 | 0.999816 | 0.999758 |
| | TESTING RESULTS | | | | | | | | | | | | | | |
| 3,10,5 | 0.009537 | 0.012052 | 0.009087 | 0.011724 | 0.006972 | 1.377630 | 1.388836 | 0.233991 | 0.519499 | 0.353514 | 0.968008 | 0.975543 | 0.998639 | 0.997652 | 0.996423 |
| 3,11,5 | 0.002138 | 0.005081 | 0.002959 | 0.004980 | 0.002827 | 0.745567 | 0.913703 | 0.153382 | 0.428707 | 0.278407 | 0.992828 | 0.989690 | 0.999557 | 0.999003 | 0.998549 |
| 3,12,5 | 0.001575 | 0.000535 | 0.002215 | 0.002132 | 0.001754 | 0.711073 | 0.314445 | 0.134448 | 0.294705 | 0.209037 | 0.994716 | 0.998915 | 0.999668 | 0.999573 | 0.999100 |
| 3,13,5 | 0.000918 | 0.001250 | 0.001631 | 0.001967 | 0.001683 | 0.485867 | 0.459264 | 0.117219 | 0.297136 | 0.207335 | 0.996920 | 0.997464 | 0.999756 | 0.999606 | 0.999136 |
| 3,14,5 | 0.000358 | 0.000473 | 0.001234 | 0.001384 | 0.000397 | 0.304171 | 0.292979 | 0.091349 | 0.198505 | 0.102452 | 0.998798 | 0.999040 | 0.999815 | 0.999723 | 0.999796 |
| 3,15,5 | 0.000210 | 0.000225 | 0.000662 | 0.000726 | 0.000326 | 0.221067 | 0.196572 | 0.073058 | 0.182743 | 0.097035 | 0.999297 | 0.999543 | 0.999901 | 0.999855 | 0.999833 |

Table 18.: Summary results of RP optimizer

| | Result Summary-RP | | | | | | | | | | | | | | |
|--------------------|-------------------|---------|---------|---------|---------|--------------|---------|---------|---------|---------|------------|---------|---------|---------|---------|
| | MSE-MINIMUM | | | | | MAPE-MINIMUM | | | | | R2-MAXIMUM | | | | |
| TRAINING (3,15,5) | 0.00796 | 0.00835 | 0.02420 | 0.02125 | 0.03124 | 1.57882 | 1.25825 | 0.46693 | 0.94288 | 0.97886 | 0.97425 | 0.98374 | 0.99663 | 0.99549 | 0.98461 |
| VALIDATION(3,15,5) | 0.00842 | 0.01067 | 0.02479 | 0.02801 | 0.03214 | 1.60613 | 1.43908 | 0.49685 | 1.13915 | 0.98235 | 0.96037 | 0.96847 | 0.99485 | 0.99207 | 0.97909 |
| TESTING (3,15,5) | 0.00895 | 0.00920 | 0.02532 | 0.02077 | 0.03591 | 1.68984 | 1.33756 | 0.48252 | 0.91747 | 1.03534 | 0.96999 | 0.98133 | 0.99621 | 0.99584 | 0.98157 |

Table 17 shows performance measures, MSE, MAPE, and R^2 , as well as the outcomes of the RProp optimizer when forecasting the surface parameters R_a , R_q , R_z , R_p , and R_v following the training of an ANN model using input data T_{on} , T_{off} , and I_p . Each row displays architecture values between 3,10,5, and 3,15,5. The first digit 3 indicates the number of neurons in the input layers. The middle digits 10 and 15, indicate the number of neurons in a hidden layer, The third numeral 5 indicates the number of neurons in the output layer. Table 18 shows lowest MSE and MAPE values and the highest R^2 value for testing, validation, and training using the best architecture (3,15,5).

Charts are prepared to study magnitude of errors between experimental and predicted surface roughness values of R_a , R_q , R_z , R_p and R_v for best optimiser during training.

4.5. Performance and regression plots

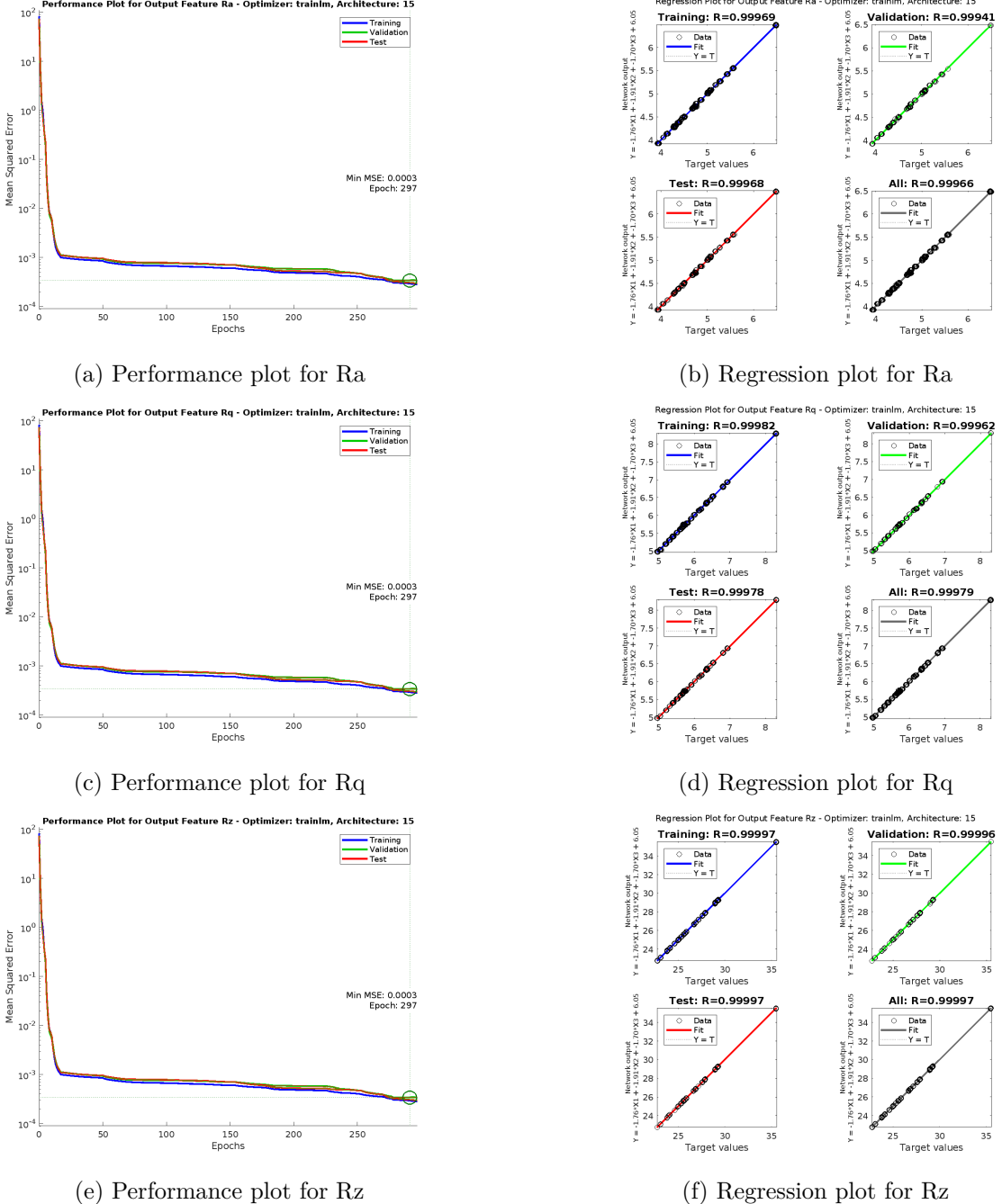


Figure 6.: Performance and regression plot for training of Ra, Rq, Rz, Rp, Rv

Figure 6a, 6c, 6e, shows the performance of ANN training for the optimizer LM with architecture (3,15,5) for roughness parameter Ra. Figure 6b, 6d, 6f, shows a regression plot of ANN training of optimizer LM with architecture (3,15,5) for roughness parameter Ra, Rq, Rz. Similar results were observed for Rp and Rv parameters.

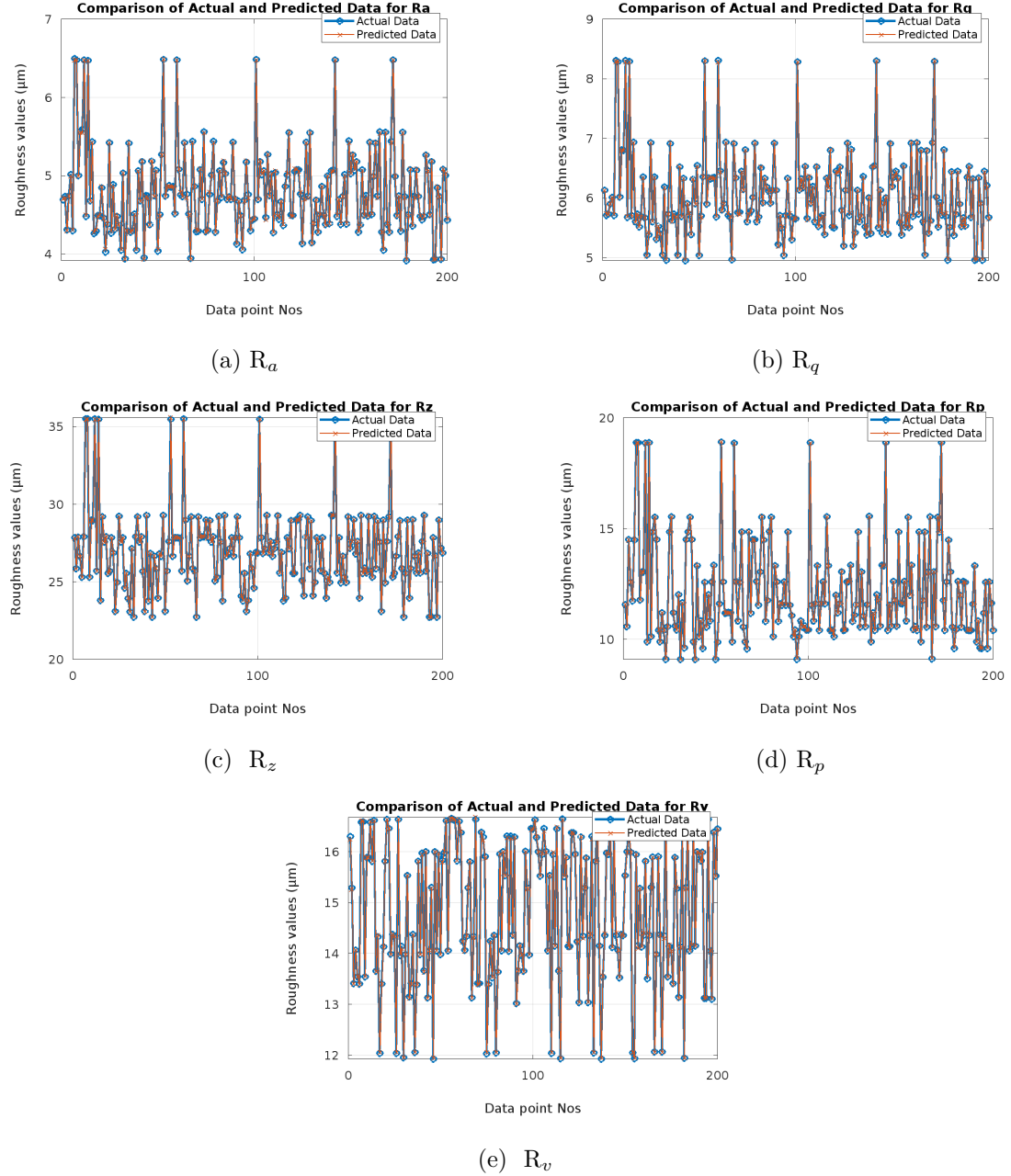


Figure 7.: comparison of actual and predicted values of (a) R_a , (b) R_q , (c) R_z , (d) R_p , (e) R_v

The Fig. 7a, 7b, 7c, 7d, 7e, gives the comparison of the results of LM optimizer for testing for architecture (3,15,5). This is the best architecture and shows the result of the best optimizer LM for testing.

4.6. Comparison of ANN results of LM, BR, RProp

Using experimental data, an artificial neural network model is created to predict R_p , R_v , R_a , R_q , and R_z . Results of MSE, MAPE, and R^2 in table 19 are compared. It is observed that the proposed model can be used to predict R_p , R_a , R_q , R_z , R_v of Dies made by the EDM process. Out of the three optimizers- LM, BR, RProp, LM performs well while predicting surface roughness parameters: R_a , R_q , R_z , R_p , R_v during training. During validation process, also LM perform well for R_a , R_z , R_p , R_v but BR performs well for R_q . During testing, using LM, gave good results while predicting R_a , R_q , R_z , and R_p , whereas, the BR optimizer gave good results while predicting R_v .

Table 19.: ANN - Results summary

| Metrics | MSE (Minimum) | | | | | MAPE (Minimum) | | | | | R^2 (Maximum) | | | | |
|----------------|---------------|---------|---------|---------|---------|----------------|---------|---------|---------|---------|-----------------|---------|---------|---------|---------|
| Roughness | Ra | Rq | Rz | Rp | Rv | Ra | Rq | Rz | Rp | Rv | Ra | Rq | Rz | Rp | Rv |
| TRAINING | | | | | | | | | | | | | | | |
| Best optimizer | LM | LM | LM | LM | LM | LM | LM | LM | LM | LM | LM | LM | LM | LM | LM |
| Metrics values | 0.00019 | 0.00019 | 0.00045 | 0.00034 | 0.00035 | 0.22421 | 0.17998 | 0.05936 | 0.11588 | 0.09217 | 0.99938 | 0.99964 | 0.99994 | 0.99993 | 0.99983 |
| VALIDATION | | | | | | | | | | | | | | | |
| Best optimizer | LM | BR | LM | LM | LM | BR | BR | LM | LM | LM | LM | BR | LM | LM | LM |
| Metrics values | 0.00019 | 0.00019 | 0.00045 | 0.00034 | 0.00035 | 0.22421 | 0.17998 | 0.05936 | 0.11588 | 0.09217 | 0.99938 | 0.99964 | 0.99994 | 0.99993 | 0.99983 |
| TESTING | | | | | | | | | | | | | | | |
| Best optimizer | LM | LM | LM | LM | BR | BR | BR | LM | LM | BR | LM | LM | LM | LM | BR |
| Metrics values | 0.00019 | 0.00019 | 0.00045 | 0.00034 | 0.00035 | 0.22421 | 0.17998 | 0.05936 | 0.11588 | 0.09217 | 0.99938 | 0.99964 | 0.99994 | 0.99993 | 0.99983 |

5. Conclusions

The experiment was conducted on dies made from EN8 material using the EDM process. Surface roughness values, viz. R_a , R_q , R_v , R_p , and R_z , are measured using a Profilometer. Comparison of results of RSM and ANN shows that ANN is superior while predicting surface roughness parameters. Results of RSM for MSE and MAPE are higher and for R^2 are lower than results of ANN during training and testing while predicting R_a , R_q , R_z , R_p , and R_v . Also, the experimental investigation revealed that the network architecture (3-15-5) gave the best results.

Experimental investigation of ANN results for the LM optimizer is superior. As MSE, MAPE values are very small and R^2 is very high, indicating the best performance, while predicting R_a , R_q , R_z , R_p , and R_v during training. During training of the ANN model using R_a , R_q , R_z , R_p , and R_v , the MSE values obtained were 0.00019, 0.00019, 0.00045, 0.00034, 0.00035, and the MAPE values obtained were 0.22421, 0.17998, 0.05936, 0.11588, 0.09217, and the R^2 values obtained were 0.99938, 0.99964, 0.99994, 0.99993, and 0.99983, respectively.

Similarly, the BR optimizer gave the best results during testing of R_v for all metrics. Also, the BR optimizer performed best while predicting R_a and R_q . This is true by considering MAPE only. All other parameters were tested using an LM optimizer and obtained good results. Similarly, during testing of R_a , R_q , R_z , and R_p , MSE values obtained were 0.00019, 0.00019, 0.00045, 0.00034, and 0.00035, and MAPE values obtained were 0.22421, 0.17998, 0.05936, 0.11588, 0.09217, and R^2 values obtained were 0.99938, 0.99964, 0.99994, 0.99993, and 0.99983, respectively. During testing, while predicting R_a , R_q , R_z , R_p , and R_v , the average values obtained were 0.00030, 0.13432, and 0.99974 for MSE, MAPE, and R^2 , respectively.

While validating, the BR optimizer gave the best result for R_q for all metrics. Also, the BR optimizer performs best for MAPE of R_a . The LM optimizer gave good results while validating the remaining parameters. During the validation process of the ANN model using R_a , R_q , R_z , R_p , and R_v , the MSE values obtained were 0.00019, 0.00019, 0.00045, 0.00034, 0.00035, and the MAPE values obtained were 0.22421, 0.17998, 0.05936, 0.11588, 0.09217, and the R^2 values obtained were .99938, 0.99964, 0.99994, 0.99993, 0.9998, respectively.

From the above paragraphs, it may be concluded that the LM optimizer gave the best performance while predicting the different surface roughness parameters using the network architecture (3-15-5).

The proposed ANN-based model finds application in the inspection of dies made out of EN8 material. Die inspection includes predicting the surface roughness parameters, such as R_z , R_p , R_q , R_a , and R_v . The method proposed in this paper will be useful in the comprehensive inspection of Dies. This will be useful in predicting the functionality of the Dies before its deployment. In the future, an effort will be made to assess the functionality of the Die by using the measured surface roughness parameters.

References

- [1] Anurag Joshi, Amit Kumar Saraf, and Ravi Kumar Goyal. Edm machining of die steel en8 and testing of surface roughness with varying parameters. *Materials Today: Proceedings*, 28:2557–2560, 2020.
- [2] M Mustafaiz Ahmad, R Davis, N Maurya, P Singh, and S Gupta. Optimization of process parameters in electric discharge machining process. *International Journal of Mechanical Engineering (IJME)*, 5(4):45–52, 2016.
- [3] Ushasta Aich and Simul Banerjee. Modeling of edm responses by support vector machine regression with parameters selected by particle swarm optimization. *Applied Mathematical Modelling*, 38(11-12):2800–2818, 2014.

- [4] C Balasubramaniyan, K Rajkumar, and S Santosh. Wire-edm machinability investigation on quaternary ni44ti50cu4zr2 shape memory alloy. *Materials and Manufacturing Processes*, 36(10):1161–1170, 2021.
- [5] Milan Kumar Das, Kaushik Kumar, Tapan Kumar Barman, and Prasanta Sahoo. Prediction of surface roughness in edm using response surface methodology and artificial neural network. *Journal of Manufacturing Technology Research*, 6(3/4):93, 2014.
- [6] C Naresh, PSC Bose, and CSP Rao. Artificial neural networks and adaptive neuro-fuzzy models for predicting wedm machining responses of nitinol alloy: Comparative study. *SN Applied Sciences*, 2:1–23, 2020.
- [7] KM Patel*, Pulak M Pandey, and P Venkateswara Rao. Determination of an optimum parametric combination using a surface roughness prediction model for edm of al₂o₃/sicw/tic ceramic composite. *Materials and Manufacturing Processes*, 24(6):675–682, 2009.
- [8] Uma Maheshwera Reddy Paturi, Suryapavan Cheruku, Venkat Phani Kumar Pasunuri, Sriteja Salike, NS Reddy, and Srija Cheruku. Machine learning and statistical approach in modeling and optimization of surface roughness in wire electrical discharge machining. *Machine Learning with Applications*, 6:100099, 2021.
- [9] TR Paul, A Saha, H Majumder, V Dey, and P Dutta. Multi-objective optimization of some correlated process parameters in edm of inconel 800 using a hybrid approach. *Journal of the Brazilian Society of Mechanical Sciences and Engineering*, 41:1–11, 2019.
- [10] BC Routara, Diptikanta Das, MP Satpathy, BK Nanda, AK Sahoo, and Shubham S Singh. Investigation on machining characteristics of t6-al7075 during edm with cu tool in steady and rotary mode. *Materials Today: Proceedings*, 26:2143–2150, 2020.
- [11] Jamal Saeedi, Matteo Dotta, Andrea Galli, Adriano Nasciuti, Umang Maradia, Marco Boccadoro, Luca Maria Gambardella, and Alessandro Giusti. Measurement and inspection of electrical discharge machined steel surfaces using deep neural networks. *Machine Vision and Applications*, 32:1–15, 2021.
- [12] Ranjit Singh, Ravi Pratap Singh, and Rajeev Trehan. Machine learning algorithms based advanced optimization of edm parameters: An experimental investigation into shape memory alloys. *Sensors International*, 3:100179, 2022.
- [13] H Varol Ozkavak, MM Sofu, B Duman, and S Bacak. Estimating surface roughness for different edm processing parameters on inconel 718 using gep and ann. *cirp j manuf sci technol* 33: 306–314, 2021.
- [14] L Yogesh, M Arunadevi, and CPS Prakash. Predicton of mrr & surface roughness in wire edm machining using decision tree and naive bayes algorithm. In *2021 International Conference on Emerging Smart Computing and Informatics (ESCI)*, pages 527–532. IEEE, 2021.
- [15] İlhan Asiltürk and Mehmet Çunkaş. Modeling and prediction of surface roughness in turning operations using artificial neural network and multiple regression method. *Expert systems with applications*, 38(5):5826–5832, 2011.
- [16] Vishal Lalwani, Priyaranjan Sharma, Catalin Iulian Pruncu, and Deepak Rajendra Unune. Response surface methodology and artificial neural network-based models for predicting performance of wire electrical discharge machining of inconel 718 alloy. *Journal of Manufacturing and Materials Processing*, 4(2):44, 2020.
- [17] Kumaresh Dey, Kanak Kalita, and Shankar Chakraborty. Prediction performance analysis of neural network models for an electrical discharge turning process. *International Journal on Interactive Design and Manufacturing (IJIDeM)*, 17(2):827–845, 2023.

- [18] Azlan Mohd Zain, Habibollah Haron, and Safian Sharif. Prediction of surface roughness in the end milling machining using artificial neural network. *Expert Systems with Applications*, 37(2):1755–1768, 2010.
- [19] Amreeta R Kaigude, Nitin K Khedkar, Vijaykumar S Jatti, Sachin Salunkhe, Robert Cep, and Emad Abouel Nasr. Surface roughness prediction of aisi d2 tool steel during powder mixed edm using supervised machine learning. *Scientific Reports*, 14(1):9683, 2024.
- [20] Angelos P Markopoulos, Dimitrios E Manolakos, and Nikolaos M Vaxevanidis. Artificial neural network models for the prediction of surface roughness in electrical discharge machining. *Journal of intelligent Manufacturing*, 19:283–292, 2008.
- [21] Liborio Cavalieri, George E Chatzarakis, Fabio Di Trapani, Maria G Douvika, Konstantinos Roinos, Nikolaos M Vaxevanidis, and Panagiotis G Asteris. Modeling of surface roughness in electro-discharge machining using artificial neural networks. *Advances in materials Research*, 6(2):169, 2017.
- [22] Dipti Kanta Das, Ashok Kumar Sahoo, Ratnakar Das, and BC Routara. Investigations on hard turning using coated carbide insert: Grey based taguchi and regression methodology. *Procedia Materials Science*, 6:1351–1358, 2014.
- [23] Arkadeb Mukhopadhyay, Tapan Kumar Barman, Prasanta Sahoo, and J Paulo Davim. Modeling and optimization of fractal dimension in wire electrical discharge machining of en 31 steel using the ann-ga approach. *Materials*, 12(3):454, 2019.

6. Supplementary information

6.1. Code availability

[Visit Github](#)

6.2. ORCID

Ghanshyam Patel  <https://orcid.org/0000-0002-5446-9424>

M.B.Kiran  <https://orcid.org/0000-0001-5855-8670>